Intracellular Localization of Proteasomal Degradation of a Viral Antigen

Luis C. Antón,* Ulrich Schubert,*‡ Igor Bacík,* Michael F. Princiotta,* Pamela A. Wearsch,* James Gibbs,* Patricia M. Day,§ Claudio Realini,‖ Martin C. Rechsteiner,‖ Jack R. Bennink,* and Jonathan W. Yewdell*

*Laboratory of Viral Diseases, National Institute of Allergy and Infectious Diseases, Bethesda, Maryland 20892; ‡Heinrich-Pette Institute, University of Hamburg, Hamburg, Germany; §Laboratory of Cellular Oncology, National Cancer Institute, Bethesda, Maryland 20892; and ‖Department of Biochemistry, University of Utah, Salt Lake City, Utah 84112

Abstract. To better understand proteasomal degradation of nuclear proteins and viral antigens we studied mutated forms of influenza virus nucleoprotein (NP) that misfold and are rapidly degraded by proteasomes. In the presence of proteasome inhibitors, mutated NP (dNP) accumulates in highly insoluble ubiquitinated and nonubiquitinated species in nuclear substructures known as promyelocytic leukemia oncogenic domains (PODs) and the microtubule organizing center (MTOC). Immunofluorescence revealed that dNP recruits proteasomes and a selective assortment of molecular chaperones to both locales, and that a similar (though less dramatic) effect is induced by proteasome inhibitors in the absence of dNP expression. Biochemical evidence is consistent with the idea that dNP is delivered to PODs/MTOC in the absence of proteasome inhibitors. Restoring proteasome activity while blocking protein synthesis results in disappearance of dNP from PODs and the MTOC and the generation of a major histocompatibility complex class I–bound peptide derived from dNP but not NP. These findings demonstrate that PODs and the MTOC serve as sites of proteasomal degradation of misfolded dNP and probably cellular proteins as well, and imply that antigenic peptides are generated at one or both of these sites.

Key words: antigen presentation • molecular chaperone • nuclear proteins proteolysis • ubiquitin/immunology • proteasome

PROTEASOMES are complex multisubunit proteases abundant in the nucleus and cytosol that function in all eukaryotic cells to degrade damaged or unwanted proteins. The major means of tagging proteins for proteasomal destruction is covalent modification by multiple chains of ubiquitin (Ub)[1] (Ciechanover, 1998). Incubation of cells with proteasome inhibitors results in the accumulation of polyubiquitinated proteins, and in most circumstances, cell death (Bogyo et al., 1997; Lee and Goldberg, 1998).

Address all correspondence to J.W. Yewdell or J.R. Bennink, Room 213, Building 4, 4 Center Drive, NIH, Bethesda, MD 20892-0440. Tel.: 301-402-4602. Fax: 301-402-7362. E-mail: jyewdell@nih.gov or jbennink@nih.gov

1. *Abbreviations used in this paper:* APL, acute PML; dNP, misfolded nucleoprotein; GFP, green fluorescent protein; LC, lactacystin; LCSM, laser confocal scanning microscope; MTOC, microtubule organizing center; NP, influenza virus nucleoprotein; NP_{pep}, NP with SIINFEKL appended to the COOH terminus; OVA, ovalbumin; PBC, primary biliary cirrhosis; PML, promyelocytic leukemia; POD, PML oncogenic domain; RAR, retinoic acid receptor; rVV, recombinant vaccinia virus; Ub, ubiquitin; zLLL, cbz-LeuLeuLeucinal.

Proteasomes participate in the generation of many of the peptides that are displayed on the cell surface in a complex with class I molecules of the major histocompatibility complex for surveillance by the immune system (York and Rock, 1996). Peptides are generated indiscriminately from host gene products and gene products of viruses and other intracellular pathogens (Pamer and Cresswell, 1998). Discrimination between self and nonself peptides is performed at the level of the antigen receptor expressed by $CD8^+$ T lymphocytes. There is sufficient plasticity in the system to enable T cell recognition of some self antigens, which accounts for the generation of most defined T cell responses to tumors.

Although there has been rapid progress in understanding the function of the proteasome-Ub system in cellular metabolism, and more specifically, its role in generating antigenic peptides, many important questions remain, including the involvement of molecular chaperones in the process, the intracellular sites of ubiquitination and proteasomal degradation, and the nature of substrates that provide antigenic peptides. In the present communication we describe findings with a metabolically unstable form of

influenza virus nucleoprotein (NP) that provide some initial answers to these questions.

Materials and Methods

Cells

143B human osteosarcoma cells lacking thymidine kinase and HeLa cells were obtained from the American Type Culture Collection and maintained in DMEM supplemented with 7.5% (vol/vol) fetal bovine serum in an air/CO_2 (91%/9%) atmosphere at 37°C. L929 cells expressing K^b from a transfected gene were maintained similarly.

Viruses

Recombinant vaccinia viruses (rVVs) were constructed by standard methodology (Chakrabarti et al., 1985) using a modified form of pSC11 with multiple cloning sites to express inserted genes under the control of the p7.5 promoter active early and late in VV replication. dNPpep was constructed by inserting an oligonucleotide encoding KEKEKNKLKRKKLENKDKKDEERNKIREE at position 333 in NP_{pep}. Green fluorescent protein (GFP) constructs were created by fusing NP_{pep} or dNP_{pep} encoding constructs with a cDNA encoding EGFP (Clontech), a red-shifted version of GFP modified by two substitutions (Phe_{64}→Leu, Ser_{65}→Thr), and 190 synonymous coding alterations to match human codon usage. For cloning convenience, sequences encoding the spacer peptide ARDPPVAT were inserted between the COOH terminus of the NP_{pep} constructs and initiating Met of GFP. Most VV infections were performed with media containing cytosine arabinoside at 40 μg/ml to limit expression to viral gene products expressed under the control of early promoters. This reduces the morphological alterations in cells induced by VV and also controls for the blockade in late VV gene expression induced by proteasome inhibitors (Antón et al., 1998).

Antibodies

Antipeptide antisera were prepared by immunizing rabbits with synthetic peptides conjugated to KLH. Peptides corresponded to PR8 NP sequences 2-12 +Cys and Cys+488-498; the extraneous Cys being used for conjugation and coupling to beads. The NH_2-terminal–specific serum was affinity purified against the synthetic peptide disulfide coupled to SulfoLink® beads (Pierce Chemical Co.) and absorbed multiple times against uninfected fixed and permeabilized cells to remove antibodies specific for cellular proteins. The COOH-terminal antiserum could be used without further purification. Monoclonal antibodies specific for the proteasome (clones MCP20 and MCP21) were generously provided by K.B. Hendil (University of Copenhagen, Copenhagen, Denmark). Human sera from primary biliary cirrhosis (PBC) patients containing anti–promyelocytic leukemia (PML) oncogenic domain (POD) antibodies were generously provided by D.B. Bloch (Harvard Medical School, Charlestown, MA) and J. Liang (NIDDK, Bethesda, MD). The colocalization of human antibody staining of PODs in TK^- cells with the anti-PML mAb was confirmed. The commercial sources of the following antibodies are as listed: poly Ub mouse mAb, clone FK2, Nippon Bio-Test Laboratories; PML mouse mAb, clone PG-M3, Santa Cruz Biotechnologies; γ-tubulin mouse mAb, clone gtu-88, Sigma Chemical Co.; HSP27 mouse mAb, clone G3.1, HSP40 rabbit Ab (SPA-400), HSP47 mouse mAb, clone M16.10A1, HSP56 mouse mAb, clone KN382/EC1, HSP60 mouse mAb, clone LK-1, HSC70 rat mAb, clone 1B5, HSP70 mouse mAb, clone C92F3A-5, HSP90, rat mAb, clone 16F1, and HSP110 rabbit Ab (SPA-1101), all from StressGen Biotechnologies.

Immunofluorescence

Cells were grown overnight on acid-cleaned, 0.17-mm-thick, 12-mm-diameter glass coverslips placed in 24-well plates, infected with virus, and incubated as indicated in the text and figure legends. At the appropriate time, cells were fixed by incubation with 3% (wt/vol) paraformaldehyde in PBS for 20 min and permeabilized by 2 min of treatment with 1% (vol/vol) NP-40 in PBS. After quenching of formaldehyde with 200 mM glycine/PBS, cells were incubated with a mixture of primary antibodies diluted in PBS supplemented with 5% (vol/vol) donkey serum, usually overnight, at 4°C, washed, and incubated for 2–8 h in the same diluent containing secondary donkey antibodies conjugated to DTAF, Texas red, or Cy5, specific for mouse, human, rabbit, or rat Ig (Jackson ImmunoResearch). Coverslips were mounted on glass slides with Fluoromount-G (Southern Biotechnology) containing 15-μm-diameter beads to prevent cell compression, and images collected with a Bio-Rad MRC1024 laser scanning confocal Zeiss Axioplan microscope, using a 63× planapochromat oil immersion objective. Controls established the specificity of fluorochrome-conjugated antibodies for their respective Igs, and that signals in green, red, and far red channels were derived from the respective fluor. Digital images were assembled using Adobe Photoshop software and printed with a Fujix Pictrography digital printer (Fuji). For cytofluorography, cells were incubated with mAbs for 30 min on ice, washed, and incubated with rabbit anti–mouse Ig conjugated to fluorescein (Dako). Cells were suspended in PBS containing ethidium homodimer (Molecular Probes), and analyzed using a FACScalibur® cytofluorograph (Becton Dickinson). Live cells were gated based on scattering properties and low ethidium homodimer staining.

Biochemical Procedures

Western Blotting. Confluent 143B cells grown in 6-well plates were infected with rVVs and incubated for 150 min and then for 360 min in the presence or absence of 20 μM cbz-LeuLeuLeucinal (zLLL). Plates were transferred to an ice bath, and subjected to a sequential extraction to prepare the nuclear matrix, according to the protocol of Staufenbiel and Deppert (1984), with the exception that all buffers contained Complete® protease inhibitor cocktail (EDTA-free; Boehringer Mannheim) and 10 μM zLLL. Equivalent amounts of samples from each step of the procedure were acetone precipitated, and precipitates resuspended in boiling SDS-PAGE sample buffer (Laemmli, 1970). Samples were also prepared from rVV-infected HeLa cells by suspending cells in ice-cold buffer containing 50 mM Tris-hydrochloride (pH 8.0), 5 mM EDTA, 100 mM NaCl, 0.5% (wt/vol) CHAPS ([3-[(3-cholamidopropyl)-dimethyl-ammonio]-1-propanesulfonate]), 0.2% (wt/vol) deoxycholate, and then mixed with an equal volume of boiling SDS-PAGE sample buffer. After electrophoresis, proteins were transferred to Immobilon P membranes (Millipore) in transfer buffer (Towbin et al., 1979) lacking SDS. Membranes were incubated overnight with TBS-Casein (Bio-Rad), and then with rabbit anti-NP antibodies, followed by peroxidase-labeled anti–rabbit IgG (Boehringer Mannheim). Blots were developed using the ECL system (Pierce Chemical Co.), and luminescence recorded by Biomax MR film (Kodak). Images were digitized by a flat bed scanner, assembled using Adobe Photoshop software, and printed with a Fujix Pictrography digital printer.

[^{35}S]Met Labeling. 143 cells infected 3 h previously were incubated in Met-free DMEM with 100 μM lactacystin (LC) for 40 min, and then radiolabeled by 5 min of incubation with [^{35}S]Met. After washing, cells were chased at 37°C for up to 120 min in Met containing DMEM. At appropriate times, 2×10^6 cells were removed to ice. Cells were incubated with 1% (vol/vol) Triton X-100 (TX100) containing buffer and centrifuged at 15,000 *g* for 10 min. Supernatants and pellets were suspended in boiling SDS-PAGE sample buffer boiled for 5 min, and analyzed by SDS-PAGE. Images of autoradiographs of the dried gels were digitized by a flat bed scanner, assembled using Adobe Photoshop software and printed with a Fujix Pictrography digital printer. The radioactivity present in dried gels was quantitated using a PhosphorImager (Molecular Devices) and the screens supplied by the manufacturer. The VV protein shown in Fig. 2 a was used as an internal standard for normalization of the amount of protein recovered from each sample.

Results

Modification of NP Results in Enhanced Generation of Antigenic Peptides

The NP from the PR8 influenza virus is a 498-residue protein that is transported to the nucleus via multiple nuclear localization sequences (Wang et al., 1997). We genetically engineered NP to contain a 29-residue sequence nearly identical to that from JAK1 kinase proposed to enhance the generation of antigenic peptides by targeting the protein to proteasomes (Realini et al., 1994). In addition, we appended to the COOH terminus a peptide corresponding to residues 257–264 from chicken ovalbumin (OVA). This

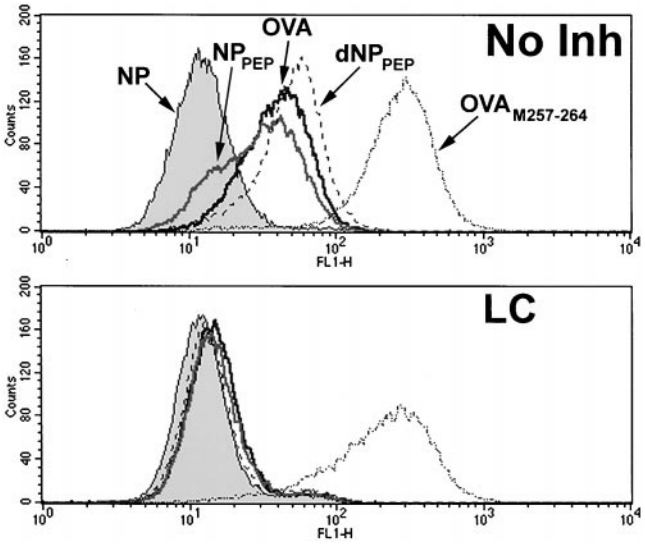

Figure 1. Proteasome-dependent production of $Ova_{257-264}$ from VV-encoded proteins. L-K^b cells incubated for 90 min in the absence (top) or presence (bottom) of 50 μM LC were infected for 8 h with the indicated rVV in the presence or absence of LC, respectively. Cells were stained with 25-D1.16 mAb and analyzed by cytofluorography.

peptide binds tightly to the H-2 K^b MHC class I molecule, and K^b–$Ova_{257-264}$ complexes can be easily quantitated cytofluorographically using a mAb (25-D1.16) specific for this complex (Porgador et al., 1997). As a control, the peptide was also expressed at the COOH terminus of wild-type NP (this is termed NP_{pep} and the other construct dNP_{pep}).

After 6 h of infection of L-K^b cells with rVVs expressing NP_{pep} or dNP_{pep}, approximately threefold more K^b–$Ova_{257-264}$ complexes were present on the surface of VV-dNP_{pep}–infected cells as determined cytofluorographically after indirect immunofluorescence (Fig. 1, top histogram). Incubation of cells with the highly specific irreversible proteasome inhibitor LC resulted in the nearly complete inhibition of complex expression from the chimeric proteins and from OVA, the parent protein (Fig. 1, bottom histogram). There was only a slight effect on cells infected with a rVV expressing $Ova_{257-264}$ as a cytosolic minigene product (a single Met is appended to the NH_2 terminus to enable efficient translation), consistent with the interpretation that LC acts by preventing proteasome liberation of $Ova_{257-264}$ (or a proteolytic intermediate) from NP_{pep}, dNP_{pep}, and OVA, and not by interfering with VV gene expression or delivery and loading of peptides onto K^b molecules.

Metabolic Stability of dNP_{pep} and NP_{pep}

Increased protein degradation is associated with enhanced generation of antigenic peptides (Tevethia et al., 1983; Townsend et al., 1988). To investigate the more efficient production of $Ova_{257-264}$ from dNP_{pep}, we examined the metabolic stability of dNP_{pep} and NP_{pep} in the presence and absence of LC. rVV-infected cells were labeled for 5 min with [^{35}S]Met and chased for up to 2 h at 37°C. Proteins present in TX100-soluble and insoluble material were separated by SDS-PAGE and the amounts of NP present in gel migrating with the expected mobility were determined by PhosphorImager analysis (Fig. 2). The total amount of NP_{pep} recovered remained nearly constant throughout the chase period, with the solubility decreasing

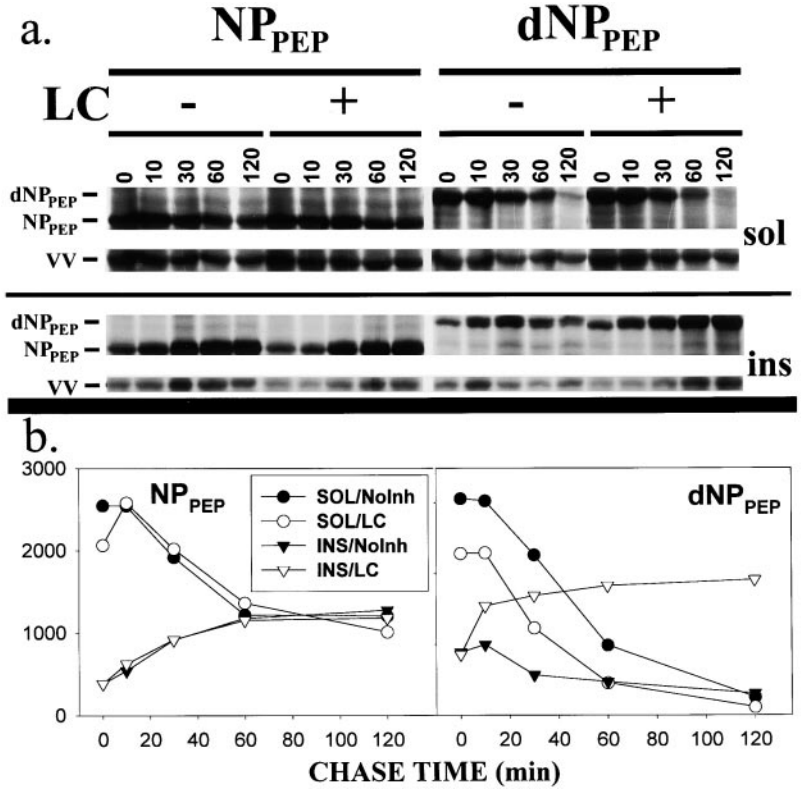

Figure 2. Proteasome-dependent degradation of dNP_{pep}. 143B cells were pulse radiolabeled with [^{35}S]Met and chased for up to 120 min at 37°C in the presence or absence of LC. Radioactive proteins soluble in 1% TX100 (sol) or insoluble (ins) were separated by SDS-PAGE and the bands corresponding to dNP_{pep} or NP_{pep} located in the dried gel (a) and quantitated (b) after normalization using a VV-encoded protein as an internal standard (indicated as VV).

in a time-dependent manner to a plateau value. This corresponds with the transport of NP_{pep} into the nucleus where it is partially TX100 insoluble. As expected, the process was unaffected by LC. By contrast, in the absence of LC, recovery of both soluble and insoluble dNP_{pep} decreased with time. Importantly, LC selectively increased the recovery of insoluble dNP_{pep}, without affecting soluble dNP_{pep}. We interpret this data to indicate that, first, insertion of the JAK1 sequence into dNP_{pep} greatly enhances its degradation by proteasomes, and, second, that the form digested by proteasomes is insoluble in TX100. These findings predict that incubation of cells with proteasome inhibitors should result in the accumulation of dNP_{pep} in cells.

Intracellular Localization of dNP_{pep}

This prediction was first confirmed by immunofluorescence of fixed and permeabilized rVV-infected cells using rabbit antibodies raised to the NH_2 terminus of unmodified NP (anti-NH_2). In the absence of proteasome inhibitors, staining of dNP_{pep} observed using a laser scanning confocal microscope (LCSM) was only slightly above background autofluorescence levels (data not shown). In the presence of either LC (data not shown) or the reversible proteasome inhibitor zLLL, dNP_{pep} was detected in three locations: weak staining of the nuclear body (excluding the nucleoli), and strong staining of small nuclear substructures (Fig. 3, first row) and, in some cells, a cytoplasmic structure that was often juxtanuclear (Fig. 3, third and fourth rows, arrows). This differs markedly from the staining pattern of NP_{pep} (Fig. 3, second row), which like wild-type NP (not shown) strongly stains the nuclear body in the presence or absence (not shown) of proteasome inhibitors.

We colocalized the focal staining of dNP_{pep} with antibodies specific for defined cellular structures. The nuclear structures colocalized with those stained by a mouse mAb (Fig. 3) or human autoimmune antibodies (see Fig. 5) specific for proteins present in PODs. PODs are enigmatic 0.3–1.0-μm-diameter macromolecular complexes comprised of >20 different proteins that are attached to the nuclear matrix (Sternsdorf et al., 1997). The cytoplasmic structure surrounded the staining obtained with a mAb specific for γ-tubulin, which identifies the pair of centrioles present at the microtubule organizing center (MTOC), the site where microtubules originate.

The accumulation of dNP_{pep} in PODs and the MTOC is not simply the result of prolonged overexpression. If cells were infected with rVV for 2–4 h in the absence of proteasome inhibitors, dNP_{pep} was detected by anti-NH_2 antibody staining in PODs and the MTOC as early as 30 min after adding zLLL in a small percentage of cells (data not shown), and by 90 min, in a high percentage of cells (see Fig. 8). In both circumstances, this represents the rapid accumulation of newly synthesized dNP_{pep}, since it did not occur if protein synthesis inhibitors were added with zLLL.

dNP_{pep} Present in PODs and MTOC Is Resistant to Detergent and High Salt Extraction and Present in High M_r Ubiquitinated Forms

PODs can be partially purified by progressive extraction designed to isolate the nuclear matrix (Staufenbiel and Deppert, 1984). This was performed biochemically and cytoimmunochemically. rVV-infected 143B cells incubated with zLLL were subjected sequentially to NP-40, DNase I, high salt, DNase I/RNAase, and then fixed with paraformaldehyde and examined using the LCSM after staining with anti-NH_2 and anti-POD antibodies. Under these conditions dNP_{pep} was easily detected in PODs and the MTOC (Fig. 4 C, arrow), whereas the low level staining of remaining NP_{pep} was in a pattern not clearly related to PODs.

Material recovered in the supernatant at each step of the extraction procedure (and a final step with Empigen BB to extract nuclear matrix–associated proteins, including those in PODs) was characterized by Western blotting using the anti-NH_2 antibodies. Almost all of the NP_{pep} expressed in the presence (Fig. 4 A) or absence (data not shown) of zLLL was recovered in the first three steps of the fractionation process. The major species recovered migrated with the expected mobility (arrowhead). In addition, faster migrating species were present that were probably generated by proteolysis during the extraction procedure.

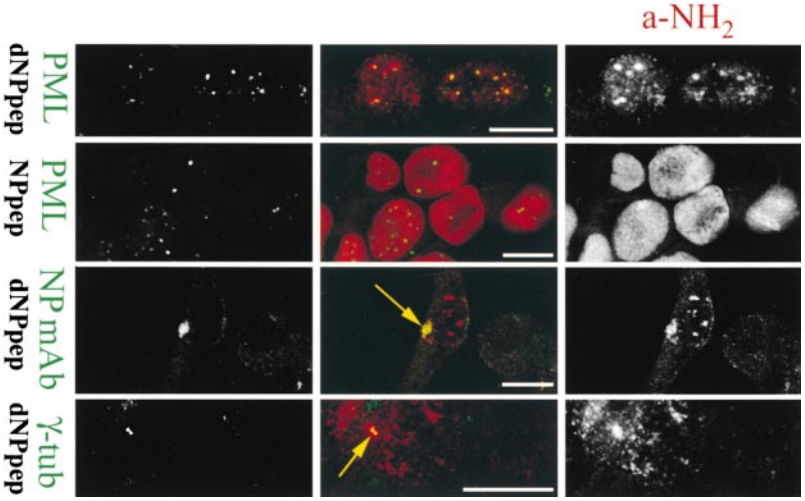

Figure 3. dNP_{pep} rescued by zLLL localizes in PODs and the MTOC. rVV-infected 143B cells were incubated for 3 h before the addition of 20 μM zLLL. After 6.5 h, cells were fixed, permeabilized, stained with the indicated antibodies, and imaged with the LCSM. The second row displays cells expressing NP_{pep}, in the first and third, cells expressing dNP_{pep}. In the bottom row, dNP_{pep} expressing cells were first extracted with 1% NP-40 and then fixed with methanol/acetone (80:20) for 15 min at −20°C to enable staining with the γ-tubulin–specific mAb. Arrows point to the MTOC. Gray-scale images on the sides are merged in the middle with the color indicated by the text describing the antibody specificity. Bar, 10 μM.

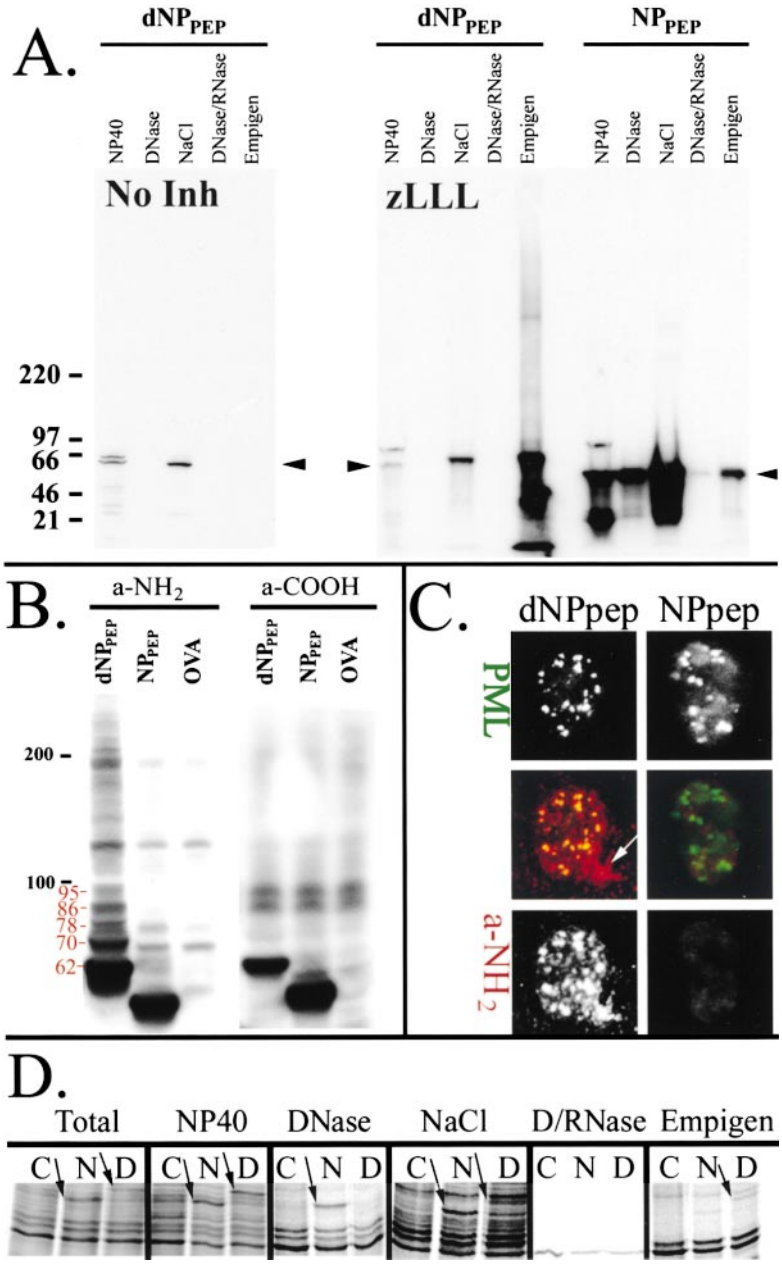

Figure 4. Fractionation and biochemical characterization of dNP$_{pep}$. (A) Extracts from rVV-infected 143B cells incubated with or without 20 μM zLLL were analyzed by Western blotting using anti-NH$_2$ antibodies. Note that the panel on the left is from a different gel than that on the right, and that the corresponding bands are more compressed. (B) HeLa cells infected with the rVV indicated for 90 min were incubated for an additional 3.5 h in the presence of 40 μM zLLL. Total cell extracts were analyzed by Western blotting using antibodies against the NH$_2$- or COOH-terminal peptides. Calculated M_r of the lower mobility bands indicated in red. (C) 143B cells expressing dNP$_{pep}$ (left) or NP$_{pep}$ (right) were extracted sequentially by NP-40, DNase I digestion, 2 M NaCl, DNase I/RNAase digestion, and then paraformaldehyde fixed, stained with anti-PML (top) or anti-NH$_2$ antibodies, and analyzed using the LCSM. Gray-scale images on the top and bottom are merged in the middle with the color indicated by the text describing the antibody specificity. The arrow points to the MTOC. (D) 143B cells infected with a control virus (C), NP$_{pep}$ (N), or dNP$_{pep}$ (D) were labeled for 5 min with [^{35}S]Met and chased for 40 min. Cells were extracted as above, and acetone precipitates were analyzed by SDS-PAGE and the radiolabeled proteins visualized using a PhosphorImager. Shown are the regions of the gel containing the proteins of interest along with control cellular and VV proteins. The intensity of total and NP-40 lysates was reduced fourfold before the 16–8 bit digital conversion to enable visualization of individual protein bands in all of the fractions. Arrows indicate NP$_{pep}$ and dNP$_{pep}$. Based on PhosphorImager quantitation (and taking into account sample recovery), 2.3-fold more NP$_{pep}$ is present in total lysates than dNP$_{pep}$, whereas 6.8-fold more dNP$_{pep}$ is recovered in the Empigen BB step.

In the absence of zLLL, the small amounts of dNP$_{pep}$ that were present behaved similarly to NP$_{pep}$, being recovered in the first and third steps of the fractionation (Fig. 4 A). In the presence of zLLL, similar amounts of dNP$_{pep}$ were recovered in these fractions, but now a large amount of dNP$_{pep}$ was recovered from the final Empigen BB extraction step. Notably, in addition to dNP$_{pep}$ that migrated with the expected mobility (arrowhead), several lower mobility species were recovered at this stage, as well as the higher mobility species that probably represent proteolytic fragments.

The nature of the lower mobility forms of dNP$_{pep}$ was examined by Western blotting of whole cell lysates of zLLL-treated HeLa cells infected with rVVs expressing dNP$_{pep}$, NP$_{pep}$, or a control protein (OVA). Using anti-NH$_2$ antibodies, the ladder-like nature of the higher M_r forms of dNP$_{pep}$ could be easily appreciated (Fig. 4 B). By contrast, only a few higher M_r forms were specifically detected (and at much lower levels) in NP$_{pep}$-expressing cells (compare to OVA-expressing cells). Calculation of the M_rs of the lower mobility dNP$_{pep}$ bands revealed an 8.1-kD difference, close to the expected M_r of Ub (8.5 kD), indicating that dNP$_{pep}$ is ubiquitinated. In the same experiment we used an antiserum from a rabbit immunized with a synthetic peptide comprising the COOH terminus of NP. This reacted strongly with unmodified dNP$_{pep}$ or NP$_{pep}$, but failed to detectably bind to any of the higher M_r forms of dNP$_{pep}$ or NP$_{pep}$. As there are no Lys residues in the COOH-terminal NP peptide to serve as targets for ubiquitination, the inability of the antibody to bind the higher

M_r forms may be due to either cleavage of a short segment of the COOH terminus, or to steric effects of ubiquitination on antibody access to the COOH terminus.

Based on these findings we conclude first that the bulk of dNP_{pep} that is normally degraded by proteasomes accumulates in TX100/NP-40–insoluble forms concentrated in PODs and the MTOC when proteasomes are inhibited, and second, that a fraction of this material is present in modified high M_r forms resulting at least in part from ubiquitination. Due to uncertainties associated with efficiencies of recovering and detecting antigens in Western blots, the ratio of ubiquitinated to nonubiquitinated dNP_{pep} cannot be determined by this method. It is worth noting, however, that at least some of the loss in the total amount of [^{35}S]Met labeled dNP_{pep} in LC-treated cells recovered over the 2-h chase period (Fig. 2 b) is due to ubiquitination with its attendant alteration in electrophoretic mobility.

Transport of dNP_{pep} to PODs/MTOC in the Absence of Proteasome Inhibitors

The failure to detect dNP_{pep} in PODs/MTOC in the absence of proteasome inhibitors raises two possibilities: the delivery of dNP_{pep} to PODs/MTOC occurs only when proteasomes are blocked; and dNP_{pep} is delivered to PODs/MTOC in the absence of proteasome inhibitors but is degraded too rapidly for cytochemical detection.

To address this issue, we labeled rVV-infected cells expressing NP_{pep} or dNP_{pep} with [^{35}S]Met for 5 min, chased for 40 min, sequentially fractionated cells as above, and analyzed the fractions by SDS-PAGE, again taking advantage of the shut down of host proteins to visualize NP and dNP_{pep} in an antibody-independent manner (Fig. 4 D). Consistent with the prior results, more NP_{pep} (~2.3-fold) is present in total cell lysates than dNP_{pep}, and the bulk of NP_{pep} is recovered in the first three fractionation steps. By contrast, less dNP_{pep} is recovered from the DNase and high salt extracts, whereas its recovery in the Empigen BB extraction step is enhanced approximately sevenfold relative to NP_{pep}. This finding is consistent with the idea that dNP_{pep} is delivered to PODs in the absence of proteasome inhibitors.

Effects of zLLL and dNP_{pep} Expression on the Distribution of Cellular Constituents of the Degradation Machinery

We next examined the effects of zLLL and dNP_{pep} expression on the distribution of cellular proteins in rVV-infected cells expressing dNP_{pep} or dNP_{pep} with GFP added to the COOH terminus, as well as cells transiently transfected with plasmids encoding the GFP-fusion proteins. dNP_{pep} was detected using either antibody staining of fixed and permeabilized cells or by GFP autofluorescence in fixed or live cells. Similar results were obtained from each of these vector/detection systems, demonstrating that the findings are not limited to VV-infected cells, and that the intracellular localization of dNP_{pep} by antibodies is not biased by fixation/permeabilization/penetration artifacts. In the interest of brevity, results will be shown only for rVV-expressed dNP_{pep}GFP. PODs were detected using sera from patients with PBC which contain Abs to PML and other POD proteins, poly Ub with a mAb (clone FK2) nonreactive with free Ub (Fujimuro et al., 1994), proteasomes using a mixture of two mAbs (MCP20 and 21) reactive with native proteasome subunits (Hendil et al., 1995), and molecular chaperones with various monoclonal and polyclonal antibodies.

In both live and fixed dNP_{pep}GFP-expressing cells treated with zLLL for 4 h, fluorescent GFP was highly concentrated in PODs and the MTOC (Fig. 5, arrows

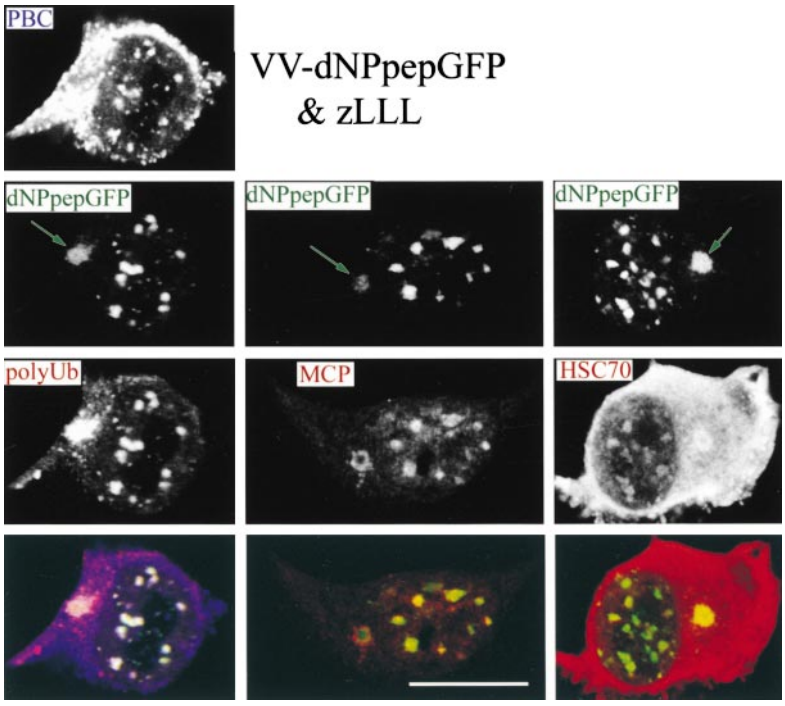

Figure 5. Effect of dNP expression on intracellular localization of components of the Ub-proteasome pathway. 143B cells infected for 4 h with VV-dNP_{pep}GFP were incubated for an additional 4 h in the presence of 10 μM zLLL, fixed, permeabilized and stained for cellular components using the antibodies indicated. dNP_{pep}GFP was located by its autofluorescence. Gray-scale images in each column are merged on the bottom with the color indicated by the text describing the antibody specificity. Arrows point to the MTOC. Bar, 10 μm.

point to the MTOC). The autofluorescence of $dNP_{pep}GFP$ indicates that the GFP domain is properly conformed, demonstrating that $dNP_{pep}GFP$ need not be completely denatured to localize to these structures. The accumulation of $dNP_{pep}GFP$ in these sites was accompanied by recruitment of poly Ub, proteasomes, and HSC70 from their normal diffuse distribution in the nucleus and cytoplasm, often to the extent that staining was reduced elsewhere in the cell (compare to Fig. 6; the distribution of proteasomes, not shown, is similar to poly Ub). While dNP_{pep} and poly Ub filled the MTOC, in many cells proteasomes and HSC70 formed a ring around MTOC. The redistribution of cellular proteins is a specific effect of inhibiting proteasomes, as similar results were obtained with LC (data not shown). A survey of mAbs specific for other molecular chaperones (data not shown) revealed HSP27 recruited PODs similarly to HSC70 and somewhat less strongly to the MTOC, and HSP70 was recruited weakly to both sites. The distribution of a number of other cytosolic chaperones (HSP110, HSP90, HSP60, HSP56, HSP47, and HSP40) was not noticeably affected by dNP_{pep} expression, and none were concentrated in either PODs or the MTOC.

In parallel experiments we examined the effects of zLLL on the distribution of the same cellular proteins in uninfected cells (Fig. 6), or VV-infected cells expressing NP_{pep}, $NP_{pep}GFP$, or GFP (data not shown). Infection with these rVVs had no major effects on the distribution of cellular proteins in untreated or zLLL-treated cells. In untreated uninfected cells, low levels of poly Ub were concentrated in a few PODs in some cells, but neither HSC70 nor proteasomes (data not shown) were concentrated in PODs. None of these cellular proteins were concentrated in the MTOC. After 6 h of zLLL treatment, poly Ub and HSC70 were clearly recruited to PODs and the MTOC. We did not detect proteasome recruitment to either the MTOC or PODs after zLLL treatment (not shown).

These data demonstrate that exposure of cells to proteasome inhibitors results in the accumulation of HSC70, HSP27, and poly Ub at PODs and the MTOC. Expression of dNP_{pep} in the presence of proteasome inhibitors accelerates and enhances these effects, and also results in recruitment of proteasomes to these structures.

Subcellular Localization of Altered Conformational States of dNP_{pep}

The conformational status of various forms of NP in cells was examined using other NP-specific antibodies. IC5-1B7 and HB65 are NP-specific mAbs that react with native NP and do not react with SDS-denatured NP in Western blots or when denatured virus is adsorbed to polyvinyl (Yewdell et al., 1981; Yewdell, J., unpublished results). In cells expressing NP or NP_{pep}, IC5-1B7 and HB65 colocalized nearly perfectly with anti-NH_2 antibodies, and the intensities of staining with the mAbs and the polyclonal serum were closely parallel, indicating that NP detected by the anti-NH_2 antibodies is largely in a folded conformation by this criterion (data not shown). The small quantities of dNP_{pep} present in cells not treated with proteasome inhibitors stained equally with the mAbs and the anti-NH_2 antiserum, indicating that conformed molecules are preferentially spared from degradation (data not shown).

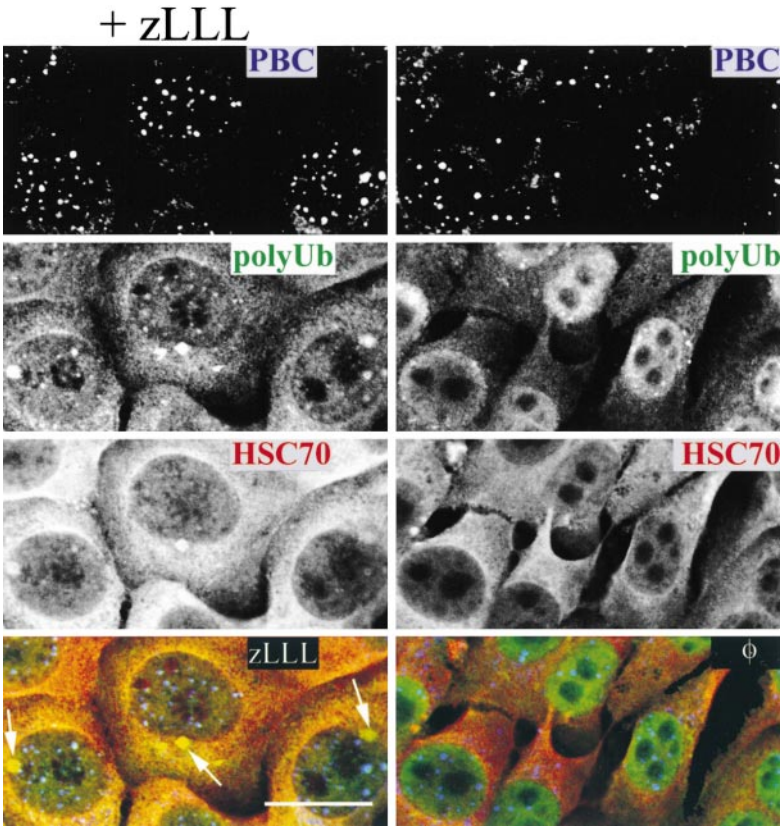

Figure 6. Effect of proteasome inhibitors on the intracellular localization of components of the Ub-proteasome pathway in uninfected cells. 143B cells were incubated for 6 h in the presence of 21 μM zLLL, fixed, permeabilized, and stained for cellular components using the antibodies indicated. Gray-scale images in each column are merged on the bottom with the color indicated by the text describing the antibody specificity. Arrows point to the MTOC. Bar, 10 μm.

In dNP_{pep}-expressing cells incubated with proteasome inhibitors, the mAbs failed to stain PODs, while intensely staining the MTOC (Fig. 3). This indicates that dNP_{pep} rescued by proteasome inhibitors exists in multiple conformations, and that most or all dNP_{pep} in PODs is at least partially unfolded.

In additional experiments (data not shown), we studied the intracellular distribution of NP constructs using the anti-COOH antiserum for immunofluorescence. When tested against VV-NP– or VV-NP_{pep}–infected cells, staining with this serum closely paralleled staining with HB65 or IC5-1B7 as detected by double immunofluorescence. When used to stain dNP_{pep} rescued by proteasome inhibitors, it strongly stained both the MTOC and PODs. Since this antiserum does not bind to ubiquitinated forms of dNP_{pep} (Fig. 4 B), this extends the biochemical data to demonstrate that nonubiquitinated dNP_{pep} is present in PODs and the MTOC.

Extension of Findings to Other Forms of NP

We examined the behavior of two other forms of rapidly degraded PR8 NP, one consisting of the first 168 residues of the protein (NP_{1-168}), the other full length NP with amino acid substitutions at residues 148 (Y→H) and 282 (G→R) (NP_{DM}). Both colocalized to PODs and the MTOC in a proteasome inhibitor–dependent manner as demonstrated using anti-NH_2 Abs, and recruited the same array of cellular proteins as dNP_{pep} (data not shown). In contrast to dNP_{pep}, NP_{DM} was detected in PODs by the HB65 mAb, demonstrating that a more conformed form of NP can localize to PODs.

It was even possible to induce wild-type NP to localize to PODs and the MTOC by exposing VV-NP–infected to cells to canavanine, an amino acid analogue of Arg that induces protein misfolding (Fig. 7). NP in PODs and the MTOC was detected by anti-COOH but not anti-NH_2 Abs, possibly due to the replacement of Arg in the NH_2-terminal peptide with canavanine (the COOH peptide used for Ab generation does not contain Arg). In addition, large amounts of NP were now detected in the cytosol, an effect possibly related to canavanine modification of the nuclear localization signal. NP in PODs and MTOC recruited poly Ub, proteasomes, and HSC70. Notably this occurred in the absence of proteasome inhibitors, suggesting that the degradation machinery (which could also be affected by canavanine) was compromised under these conditions, either as a result of having to cope with vast quantities of proteins misfolded by incorporation of canavanine, or canavanine-induced modifications in the machinery.

Together, these findings indicate that, first, that the effects with dNP_{pep} are not due to unique features of the protein conferred by the JAK1 sequence but are a general feature of misfolded PR8 NP, and, second, that similar effects can occur in the absence of proteasome inhibitors.

Proteasome-dependent In Situ Degradation of dNP_{pep}

The accumulation of dNP_{pep} in PODs and the MTOC in proteasome-inactivated cells suggested that these structures serve as sites for proteasome-mediated destruction of dNP_{pep}. To test this idea, TK^- cells were infected with VV-dNP_{pep} GFP for 4 h to maximize the rate of dNP_{pep} translation, incubated with zLLL for 90 min to accumulate a small but detectable amount of dNP_{pep} in a high percent-

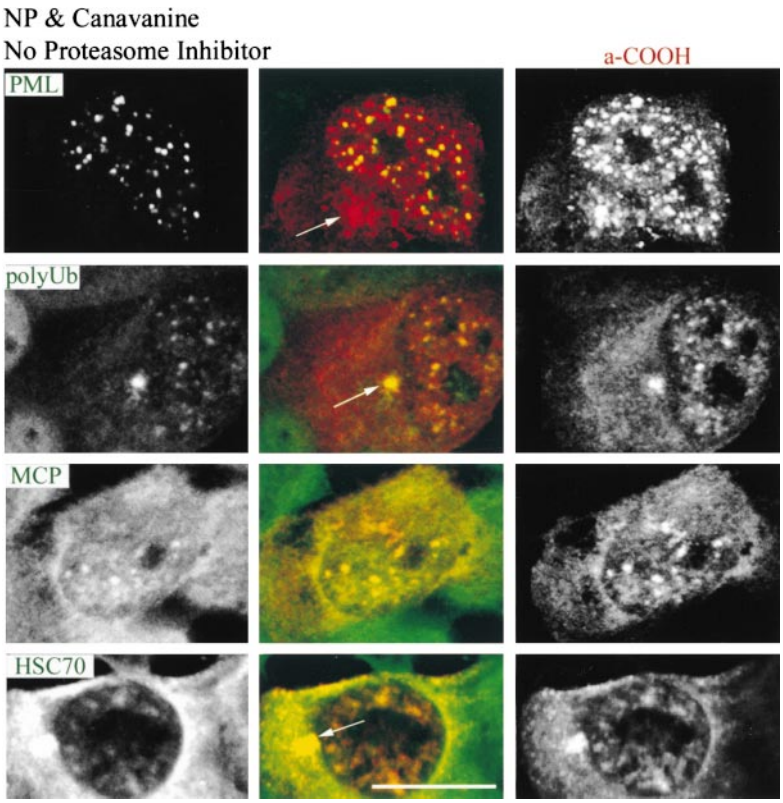

Figure 7. Effect of canavanine on intracellular localization of NP and cellular proteins. 143B cells infected for 2 h with VV-NP were incubated for an additional 6 h in the presence of 15 mM canavanine. Cells were fixed, permeabilized, and stained with the antibodies indicated. NP stained by anti-COOH antisera is shown in the right column. Gray-scale images on the left and right are merged in the middle column with the color indicated by the text describing the antibody specificity. Arrows point to the MTOC. Bar, 10 μm.

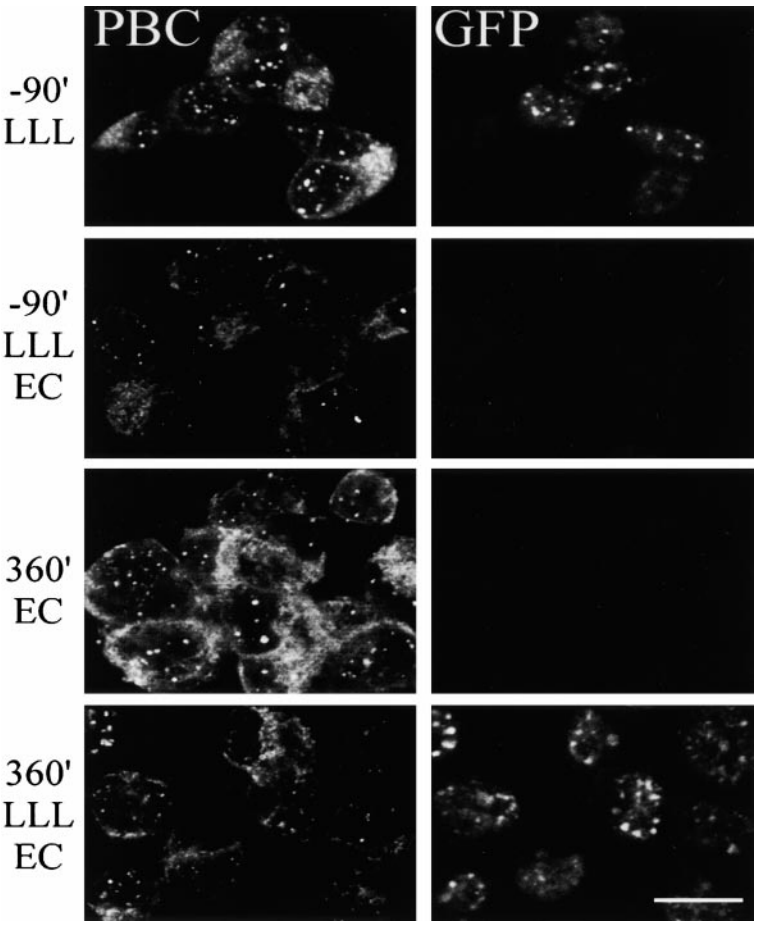

Figure 8. Proteasome-mediated in situ degradation of dNP_{pep} and generation of antigenic peptides. 143B cells infected for 4 h with VV-dNP_{pep}GFP were incubated for an additional 90 min in the presence of 10 μM zLLL in the absence (−90′ zLLL) or presence of protein synthesis inhibitors emetine (25 μM) and cycloheximide (25 μM) (−90′ zLLL EC) and then fixed, or washed, and incubated for 4 h in protein synthesis inhibitors in the absence (240′ EC) or presence of zLLL (240′ zLLL EC) and then fixed. Cells were permeabilized and stained using PBC antiserum. dNP_{pep}GFP was located by its autofluorescence. Bar, 10 μm.

age of cells, and then for 4 h in the absence of zLLL but in the presence of protein synthesis inhibitors to shut off additional dNP_{pep} synthesis (Fig. 8). After 90 min in zLLL, dNP_{pep} GFP was detected in PODs and the MTOC in most cells. Over the 4-h reversal period, dNP_{pep}GFP nearly completely disappeared (similar results were obtained in other experiments in which dNP_{pep} was detected using anti-NH_2 Abs; data not shown). This process was dependent on active proteasomes, since dNP_{pep}GFP persisted in similar quantities in PODs and the MTOC if cells were incubated with zLLL and the protein synthesis inhibitors. Based on these findings, we conclude that PODs and the MTOC serve as sources of substrates for proteasomes, and given the recruitment of proteasomes to these sites, are likely to represent sites of proteasome digestion.

We next related these findings to antigen processing. K^b was expressed in TK^- cells by coinfection with a rVV expressing K^b and mouse β_2-microglobulin, and the expression of cell surface K^b–$Ova_{257-264}$ complexes quantitated cytofluorographically after indirect staining with the 25-D1.16 mAb (Fig. 9). Levels of background staining were controlled for by infection with VV-NP. As with L-K^b cells (Fig. 1), K^b–$Ova_{257-264}$ complexes are produced more efficiently from dNP_{pep} than NP_{pep}; in this case the difference is even more pronounced (six- versus threefold increase in mean fluorescence). To correlate the disappearance of dNP_{pep} from PODs and the MTOC with proteasome mediated generation of $Ova_{257-264}$, cells were infected for 4 h in the continuous presence of zLLL, washed, and incubated for 4 h in the presence of protein synthesis inhibitors without (EC) or with zLLL (zLLL EC). In the continued presence of zLLL (zLLL EC) no complexes were generated from dNP_{pep} or NP_{pep}, since levels of staining of VV-NP–, VV-NP_{pep}–, and VV-dNP_{pep}–infected cells were identical. As described above (Fig. 1), zLLL had little effect on the generation of complexes by cells expressing the cytosolic minigene product, $Ova_{M257-264}$. Removal of zLLL in the presence of protein synthesis inhibitors was accompanied by the generation of a signal in dNP_{pep}-expressing cells above the staining of NP-expressing cells (EC). Although the shift in the curve is relatively small, it represents 31% of the signal obtained in the continuous absence of inhibitors (no inhibitor), and in absolute terms, roughly 1,000 K^b–$Ova_{257-264}$ complexes, which is more than sufficient for triggering most T cells. The effectiveness of the protein synthesis inhibitors is clearly demonstrated by the background staining of cells treated with inhibitors from the initiation of the infection (EC start), even if cells were infected with the rVV expressing the cytosolic minigene product. In contrast to results with dNP_{pep}, K^b–$Ova_{257-264}$ complexes were not generated from NP_{pep} upon removal of zLLL. These findings indicate that removal of zLLL from cells allows proteasomes to generate peptides from the dNP_{pep} that accumulates in the cells (but not from NP_{pep}), and is consistent with the idea the peptides (or their precursors) are generated at PODs, the MTOC, or at both of these locations.

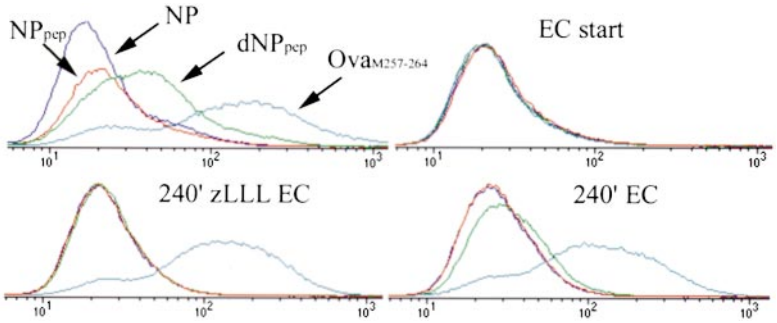

Figure 9. Antigenic peptides are generated from a pool of dNP$_{pep}$ accumulated in the presence of proteasome inhibitor. 143B cells were coinfected with a rVV expressing K^b and mouse β_2m and a rVV expressing the protein indicated. Cells were infected for 4 h in the presence of 10 μM zLLL to prevent the generation of K^b–Ova$_{257-264}$ complexes, washed, and incubated for 4 h in protein synthesis inhibitors in the presence (bottom left histogram) or absence (bottom right histogram) of zLLL. As controls, cells were incubated for 8 h in the absence of inhibitors (top left histogram) or in the presence of protein synthesis inhibitors (top right histogram). Cells were indirectly stained with the 25-D1.16 mAb to quantitate the number of cell surface K^b-Ova$_{257-264}$ complexes.

Discussion

We studied the fate of dNP$_{pep}$ as a model protein and class I–restricted antigen with a nuclear localization sequence that is ubiquitinated and degraded by proteasomes. Blocking proteasomal digestion results in the accumulation of dNP$_{pep}$ in a highly insoluble form, a portion of which is ubiquitinated. Immunofluorescence with a peptide-specific antiserum that does not detectably react with ubiquitinated substrate reveals that nonubiquitinated dNP$_{pep}$ is present at both the MTOC and PODs. The substrate-dependent enhanced recruitment of poly Ub to these structures clearly indicates that Ub-conjugated dNP is also present. This, together with the substrate-dependent recruitment of HSC70, which is required for the in vitro polyubiquitination of some proteins (Bercovich et al., 1997), is consistent with the following model: denatured dNP$_{pep}$ is chaperoned by HSC70 (and/or HSP27) to PODs and the MTOC, where it becomes an insoluble substrate for polyubiquitination and is degraded in situ by proteasomes. Several lines of evidence clearly indicate that complete denaturation of NP is not necessary for its delivery to PODs and the MTOC.

The idea that polyubiquitination of misfolded NP occurs at these sites is favored by several considerations. First, given the low solubility of ubiquitinated dNP$_{pep}$, its destruction at its site of ubiquitination would bypass the need for special mechanisms to transport it to another cellular site for disposal. Second, the rapid diffusion of GFP-tagged proteasomes visualized in viable cells (Reits et al., 1997) is fully consistent with a "search and destroy" capability for proteasomes. Third, and most directly, we have found that prolonged treatment with proteasome inhibitors (>2 h) reduces the ability of cells to polyubiquitinate proteins (our unpublished results), presumably due to a decrease in the free Ub pool (Mimnaugh et al., 1997). Limiting levels of free Ub would account, first, for the failure of cells to completely ubiquitinate dNP$_{pep}$ at PODs and the MTOC, and, second, for the plateau observed in the level of unmodified dNP$_{pep}$ recovered from LC-treated cells after pulse radiolabeling (Fig. 2 b).

We believe that a subset of cellular proteins behaves similarly to dNP$_{pep}$, since polyubiquitin and HSC70 are recruited to PODs and the MTOC of uninfected cells treated with proteasome inhibitors. Clearly, however, the effect is much less dramatic. This is not surprising given that in VV-infected cells infected for 2 h onwards, dNP$_{pep}$ represents ~5–10% of all newly synthesized protein, and that most of it denatures rapidly after synthesis. This quantitative difference probably accounts for the failure of proteasome inhibitors to recruit proteasomes to PODs and the MTOC in cells not expressing dNP$_{pep}$.

There is a considerable body of work relevant to these findings. Wojcik et al. (1996) reported that treating cells with proteasome inhibitors results in the accumulation of proteins (including proteasomes and Ub) at the MTOC: sufficient in fact to enable preferential staining of the MTOC in fixed cells with the protein stain amido black. Terming these structures "proteolysis centers," they proposed that normal degradation of proteins occurs in this location. These findings were extended recently by Johnston et al. (1998), who demonstrated the presence of ubiquitinated proteasome substrates (misfolded forms of integral membrane proteins exported from the ER) at the same location (termed "aggresomes" by these authors) in the absence of proteasome inhibitors.

We extend these findings by demonstrating that: proteins with a nuclear localization sequence can also be degraded in proteolysis centers/aggresomes; proteins destined for destruction in the MTOC can retain at least portions of their native structure as indicated by binding to conformation-specific antibodies, or in the case of GFP fusion proteins, maintenance of autofluorescence; specific molecular chaperones are involved in the process; polyubiquitin may be added to substrates at this site; and substrates present in the MTOC are degraded by proteasomes.

The last four points apply also to PODs, providing the first conclusive evidence that these structures serve as a site for proteasomal degradation of ubiquitinated proteins, which as we argue above, is probably secondary to its serving as a site ubiquitination of denatured proteins. PODs have been implicated in a number of cellular processes, including tumorigenicity, apoptosis, and viral replication (Sternsdorf et al., 1997). Herpesviruses, adenoviruses, and papilloma viruses all encode proteins that localize to PODs, in some cases, disrupting the PODs. In addition to PML (the "P" in PODs), other examples of the 20^+ known inhabitants of PODs include Sp100, HAUSP, and SUMO-1

(also known as PIC1). Significantly, both SUMO-1 and particularly HAUSP are related to the Ub-proteasome pathway. SUMO-1 is a Ub homologue that covalently modifies both PML and Sp100. Unlike Ub however, SUMO-1 modification appears to mainly affect the localization of its substrates and not their degradation, as both PML and Sp100 are localized to PODs only in their modified forms which are metabolically stable (as are other SUMO-1–modified proteins) (Saitoh et al., 1997). When used as an alternative for Ub, SUMO-1 is even known to prevent proteasomal degradation of proteins (Desterro et al., 1998). HAUSP is a Ub-dependent hydrolase, that removes Ub, but not SUMO-1 from substrates (Everett et al., 1998), and its presence in PODs is consistent with the idea that PODs serve as a center for protein ubiquitination and deubiquitination.

A chromosomal translocation characteristic for acute PML (APL) results in the creation of a fusion protein comprised of PML and the retinoic acid receptor α (RAR^{α}). The PML-RAR^{α} fusion protein acts as a dominant negative mutant, disrupting the integrity of PODs. Exposure of APL cells to retinoic acid returns the cells to a nontransformed phenotype concomitantly with the reformation of PODs and the degradation of the fusion protein (Daniel et al., 1993; Dyck et al., 1994; Weis et al., 1994). Alternatively, As_2O_3 treatment of normal or APL cells results in the recruitment of both PML and PML-RAR^{α} to PODs as well as their degradation (Zhu et al., 1997). The retinoic acid–induced degradation of PML-RAR^{α} is blocked by LC, implicating proteasomes in the process (Yoshida et al., 1996). Our findings are consistent with the idea that these proteins are degraded in PODs.

Everett et al. (1998) have shown that herpes simplex virus–induced destruction of PODs is mediated by the viral protein Vmw110 and is blocked by proteasome inhibitors. Vmw110 induces the proteasome-mediated destruction of PML and nuclear protein kinase. Vmw110 binds to HAUSP, but this is not required for its localization to PODs, or POD disruption of destruction of the kinase (Parkinson et al., 1999). These findings again support our conclusion that PODs serve as a general site of proteasome degradation, but Vmw110 probably induces proteasome degradation in multiple cellular sites, since Vmw110 mutants that do not localize to PODs can induce kinase degradation (Everett et al., 1999).

The involvement of PODs in the degradation of misfolded proteins also helps explain findings regarding mutant alleles of ataxin 1 that encode multiple copies of a polyglutamine domain present in the normal protein. These alleles are associated with a variety of inherited diseases of the nervous system. Ataxin 1 is normally present in small nuclear dots distinct from PODs. Mutant forms of ataxin 1 expressed in the absence of proteasome inhibitors are present in POD-like structures that contain PML and recruit Ub, proteasomes, HSP70, and HSP40 (Skinner et al., 1997; Cummings et al., 1998). It is uncertain to what extent ataxin versus other polyglutamine-containing proteins recruited into ataxin-initiated structures accounts for the recruitment of Ub, proteasomes, and chaperones (Perez et al., 1998). Our findings suggest that one (or more) of these misfolded proteins is recruited to PODs in association with HSP40 and HSP70, where it is polyubiquitinated but for some reason cannot be degraded by proteasomes, similar to what we describe for NP synthesized in the presence of canavanine.

Finally, we have linked the destruction of dNP_{pep} in PODs and the MTOC to the generation of an antigenic peptide present in the protein. Given that all protein synthesis occurs in the cytosol, and that nuclear and ER proteins are commonly transported to the cytosol for degradation (Ciechanover, 1998), the MTOC is probably a more general site of proteasome-mediated peptide generation, whereas peptide generation at PODs is expected to be limited largely to the subset of proteins located in the nucleus. It should be noted that the inner portion of the nuclear membrane forms part of the ER, and that peptides generated in the nucleus would not necessarily need to be delivered to the cytosol to access TAP (the MHC-encoded transporter that delivers class I ligands to the ER).

Due to the low efficiency of antigen processing, we cannot be certain that peptides are generated from dNP_{pep} accumulated at PODs/MTOC and not from lesser amounts of antigen present elsewhere in the cell. Given the function of the MTOC as proteolytic centers/aggresomes, however, it would be surprising if this were not a common site of peptide generation. Regarding PODs, there are several published findings that would support a role in antigen processing, perhaps even a specialized role in regulating the process. First, the expression of PML and other POD constituent proteins is enhanced by exposure of cells to interferons, which increase the expression of genes encoding class I molecules and the other dedicated components of the class I–processing pathway (Sternsdorf et al., 1997). Second, PML itself has been directly implicated in the regulation of antigen processing, as modifications in PML that disrupt PODs result in decreased transcription of antigen-processing genes (Zheng et al., 1998). Together with our findings, these observations suggest the following hypothesis: a signal emanating from ubiquitination/proteolysis occurring at PODs is involved in a positive feedback loop that regulates antigen processing gene transcription.

We are grateful to Drs. Bloch, Hendil, and Liang for their generous gifts of antibodies. Bethany Buschling provided outstanding technical assistance.

Submitted: 3 February 1999
Revised: 26 April 1999
Accepted: 4 June 1999

References

Antón, L.C., H.L. Snyder, J.R. Bennink, A. Vinitsky, M. Orlowski, A. Porgador, and J.W. Yewdell. 1998. Dissociation of proteasomal degradation of biosynthesized viral proteins from generation of MHC class I-associated antigenic peptides. *J. Immunol.* 160:4859–4868.

Bercovich, B., I. Stancovski, A. Mayer, N. Blumenfeld, A. Laszlo, A.L. Schwartz, and A. Ciechanover. 1997. Ubiquitin-dependent degradation of certain protein substrates in vitro requires the molecular chaperone Hsc70. *J. Biol. Chem.* 272:9002–9010.

Bogyo, M., M. Gaczynska, and H.L. Ploegh. 1997. Proteasome inhibitors and antigen presentation. *Biopolymers.* 43:269–280.

Chakrabarti, S., K. Brechling, and B. Moss. 1985. Vaccinia virus expression vector: coexpression of β-galactosidase provides visual screening of recombinant virus plaques. *Mol. Cell. Biol.* 5:3403–3409.

Ciechanover, A. 1998. The ubiquitin-proteasome pathway: on protein death and cell life. *EMBO (Eur. Mol. Biol. Organ.) J.* 17:7151–7160.

Cummings, C.J., M.A. Mancini, B. Antalffy, D.B. DeFranco, H.T. Orr, and H.Y. Zoghbi. 1998. Chaperone suppression of aggregation and altered subcellular proteasome localization imply protein misfolding in SCA1. *Nat. Genet.* 19:148–154.

Daniel, M.T., M. Koken, O. Romagne, S. Barbey, A. Bazarbachi, M. Stadler, M.C. Guillemin, L. Degos, C. Chomienne, and H. de The. 1993. PML protein expression in hematopoietic and acute promyelocytic leukemia cells. *Blood*. 82:1858–1867.

Desterro, J.M., M.S. Rodriguez, and R.T. Hay. 1998. SUMO-1 modification of IkappaBalpha inhibits NF-kappaB activation. *Mol. Cell.* 2:233–239.

Dyck, J.A., G.G. Maul, W.H.J. Miller, J.D. Chen, A. Kakizuka, and R.M. Evans. 1994. A novel macromolecular structure is a target of the promyelocyte-retinoic acid receptor oncoprotein. *Cell.* 76:333–343.

Everett, R.D., P. Freemont, H. Saitoh, M. Dasso, A. Orr, M. Kathoria, and J. Parkinson. 1998. The disruption of ND10 during herpes simplex virus infection correlates with the Vmw110- and proteasome-dependent loss of several PML isoforms. *J. Virol.* 72:6581–6591.

Everett, R.D., M. Meredith, and A. Orr. 1999. The ability of herpes simplex virus type 1 immediate-early protein Vmw110 to bind to a ubiquitin-specific protease contributes to its roles in the activation of gene expression and stimulation of virus replication. *J. Virol.* 73:417–426.

Fujimuro, M., H. Sadada, and H. Yokosawa. 1994. Production and characterization of monoclonal antibodies specific to multi-ubiquitin chains of polyubiquitinated proteins. *FEBS Lett.* 349:173–180.

Hendil, K.B., P. Kristensen, and W. Uerkvitz. 1995. Human proteasome analysed with monoclonal antibodies. *Biochem. J.* 305:245–252.

Johnston, J.A., C.L. Ward, and R.R. Kopito. 1998. Aggresomes: a cellular response to misfolded proteins. *J. Cell Biol.* 143:1883–1898.

Laemmli, U.K. 1970. Cleavage of structural proteins during the assembly of the head of bacteriophage T_4. *Nature.* 227:680–685.

Lee, D.H., and A.L. Goldberg. 1998. Proteasome inhibitors: valuable new tools for cell biologists. *Trends Cell Biol.* 8:397–403.

Mimnaugh, E.G., H.Y. Chen, J.R. Davie, J.E. Celis, and L. Neckers. 1997. Rapid deubiquitination of nucleosomal histones in human tumor cells caused by proteasome inhibitors and stress response inducers: effects on replication, transcription, translation, and the cellular stress response. *Biochemistry*. 36:14418–14429.

Pamer, E., and P. Cresswell. 1998. Mechanisms of MHC class I–restricted antigen processing. *Annu. Rev. Immunol.* 16:323–358.

Parkinson, J., S.P. Lees-Miller, and R.D. Everett. 1999. Herpes simplex virus type 1 immediate-early protein Vmw110 induces the proteasome-dependent degradation of the catalytic subunit of DNA-dependent protein kinase. *J. Virol.* 73:650–657.

Perez, M.K., H.L. Paulson, S.J. Pendse, S.J. Saionz, N.M. Bonini, and R.N. Pittman. 1998. Recruitment and the role of nuclear localization in polyglutamine-mediated aggregation. *J. Cell Biol.* 143:1457–1470.

Porgador, A., J.W. Yewdell, Y. Deng, J.R. Bennink, and R.N. Germain. 1997. Localization, quantitation, and in situ detection of specific peptide-MHC class I complexes using a monoclonal antibody. *Immunity*. 6:715–726.

Realini, C., S.W. Rogers, and M. Rechsteiner. 1994. Proposed roles in protein-protein association and presentation of peptides by MHC class I receptors. *FEBS Lett.* 348:109–113.

Reits, E.A.J., A.M. Benham, B. Plougastel, J. Neefjes, and J. Trowsdale. 1997. Dynamics of proteasome distribution in living cells. *EMBO (Eur. Mol. Biol. Organ.) J.* 16:6087–6094.

Saitoh, H., R.T. Pu, and M. Dasso. 1997. SUMO-1: wrestling with a new ubiquitin-related modifier. *Trends Biochem. Sci.* 22:374–376.

Skinner, P.J., B.T. Koshy, C.J. Cummings, I.A. Klement, K. Helin, A. Servadio, H.Y. Zoghbi, and H.T. Orr. 1997. Ataxin-1 with an expanded glutamine tract alters nuclear matrix-associated structures. *Nature.* 389:971–974.

Staufenbiel, M., and W. Deppert. 1984. Preparation of nuclear matrices from cultured cells: subfractionation of nuclei in situ. *J. Cell Biol.* 98:1886–1894.

Sternsdorf, T., T. Grotzinger, K. Jensen, and H. Will. 1997. Nuclear dots: actors on many stages. *Immunobiology*. 198:307–331.

Tevethia, S., M. Tevethia, A. Lewis, V. Reddy, and S. Weissman. 1983. Biology of simian virus 40 (SV40) transplantation antigen (TrAg). IX. Analysis of TrAg in mouse cells synthesizing truncated SV40 large T antigen. *Virology*. 128:319–330.

Towbin, H., T. Staehelin, and J. Gordon. 1979. Electrophoretic transfer of proteins from polyacrylamide gels to nitrocellulose sheets: procedure and some applications. *Proc. Natl. Acad. Sci. USA*. 76:4350–4354.

Townsend, A., J. Bastin, K. Gould, G. Brownlee, M. Andrew, B. Coupar, D. Boyle, S. Chan, and G. Smith. 1988. Defective presentation to class I–restricted cytotoxic T lymphocytes in vaccinia-infected cells is overcome by enhanced degradation of antigen. *J. Exp. Med.* 168:1211–1224.

Wang, P., P. Palese, and R.E. O'Neill. 1997. The NPI-1/NPI-3 (karyopherin α) binding site on the influenza A virus nucleoprotein NP is a nonconventional nuclear localization signal. *J. Virol.* 71:1850–1856.

Weis, K., S. Rambaud, C. Lavau, J. Jansen, T. Carvalho, M. Carmo-Fonseca, A. Lamond, and A. Dejean. 1994. Retinoic acid regulates aberrant nuclear localization of PML-RAR alpha in acute promyelocytic leukemia cells. *Cell.* 76:345–356.

Wojcik, C., D. Schroeter, S. Wilk, J. Lamprecht, and N. Paweletz. 1996. Ubiquitin-mediated proteolysis centers in HeLa cells: indication from studies of an inhibitor of the chymotrypsin-like activity of the proteasome. *Eur. J. Cell Biol.* 71:311–318.

Yewdell, J.W., E. Frank, and W. Gerhard. 1981. Expression of influenza A virus internal antigens on the surface of infected P815 cells. *J. Immunol.* 126: 1814–1819.

York, I., and K.L. Rock. 1996. Antigen processing and presentation by the class I major histocompatibility complex. *Annu. Rev. Immunol.* 14:369–396.

Yoshida, H., K. Kitamura, K. Tanaka, S. Omura, T. Miyazaki, T. Hachiya, R. Ohno, and T. Naoe. 1996. Accelerated degradation of PML-retinoic acid receptor alpha (PML-RARA) oncoprotein by all-trans-retinoic acid in acute promyelocytic leukemia: possible role of the proteasome pathway. *Cancer Res.* 56:2945–2948.

Zheng, P., Y. Guo, Q. Niu, D.E. Levy, J.A. Dyck, S. Lu, L.A. Sheiman, and Y. Liu. 1998. Proto-oncogene PML controls genes devoted to MHC class I antigen presentation. *Nature.* 396:373–376.

Zhu, J., M.H. Koken, F. Quignon, M.K. Chelbi-Alix, L. Degos, Z.Y. Wang, Z. Chen, and H. de The. 1997. Arsenic-induced PML targeting onto nuclear bodies: implications for the treatment of acute promyelocytic leukemia. *Proc. Natl. Acad. Sci. USA*. 94:3978–3983.